Talanta 83 (2010) 42–47

Contents lists available at ScienceDirect

Talanta

journal homepage: www.elsevier.com/locate/talanta

A label-free electrochemical immunoassay for IgG detection based on the electron transfer

Li-Ping Qiu [a], Cun-Chang Wang [b], Peng Hu [a], Zai-Sheng Wu [a,*], Guo-Li Shen [a], Ru-Qin Yu [a,*]

[a] State Key Laboratory for Chemo/Biosensing and Chemometrics, College of Chemistry and Chemical Engineering, Hunan University, Changsha, PR China
[b] Department of Chemistry, Xiangnan University, Chenzhou 423000, PR China

ARTICLE INFO

Article history:
Received 17 June 2010
Received in revised form 19 August 2010
Accepted 24 August 2010
Available online 29 September 2010

Keywords:
Label-free
Electrochemistry
Immunoassay
Electron transfer
Methylene blue
Gold nanoparticles

ABSTRACT

In this study, a highly selective, label-free electrochemical immunoassay strategy based on the charge transport through the multilayer films associated with the electrocatalytic reduction of $[Fe(CN)_6]^{3-}$ is proposed using human immunoglobulin G (human IgG) as the model analyte. The antibody–antigen complex formed on the sensing interface can efficiently induce change of the surface charge characteristics, the conductivity of multilayer film and/or electron transfer distance, resulting in an immunoreaction signal. The current reduction is proportional to the amount of analyte. Under the optimized experimental conditions, the proposed sensing strategy provides a linear dynamic range from 10 to 10^4 ng mL^{-1} and a detection limit of 3 ng mL^{-1}, indicating an improved analytical performance. This possibly makes it a potential alternative in bioanalysis of proteins and other molecules.

1. Introduction

Protein, as bioorganic molecule, plays a vitally important role in the life of human being. The determination of protein has become a hot topic for scientists in the era of proteomics. Thousands of analyses [1–3] having been developed, among which, the antibody-based immunoassay [4–6] attracted much attention, due to the routine tools, high selectivity and sensitivity. Enzyme linked immunosorbent assay (ELISA) [7,8] as the conventional immunoassay has been commonly used in clinical and environmental monitoring. However, it is often subject to a long assay time, high background noise and complex operation. An attractive alternative is the immunosensor [9,10], which has many striking advantages, such as simple pretreatment, low cost, high sensitivity, non-essential separation, miniaturization, and so on. Generally, immunosensor is divided into two categories: immunosensor with labels and label-free immunosensor, most of the labeled immunosensors [11,12] described to date rely on the use of different enzymes attached to biomolecules that catalyze the amplification reaction. However, the activity of the prepared conjugates must be carefully controlled due to the intrinsic instability of enzymes, and the additional procedures and external reagents must be involved. Faced with this dilemma, label-free immunoassay [13–16] has received increasing interests, due to its intrinsic superiority. Gold nanoparticles (GNPs) [17–19] are particularly attractive for biology, due to their easy preparation, good biocompatibility, chemical stability and great surface area-to-volume ratio. When used as the assembly interface, GNPs are able to increase the loading amounts and retain the bioactivity of the biomolecules, and then improve the response performance of the biosensors. Therefore, the gold nanoparticles provide a bioactive interface for the fabrication of the third-generation biosensor without electronic media.

Thionine (TH) [20–22] as a redox dye, can undergo electropolymerization at an appropriate potential on the gold electrode surface. The polythionine (PTH) films not only provide a stable sensing matrix with abundant amino groups, but also improve the conductivity of the interface, improving the sensitivity of the analytical system.

In this study, a highly selective, label-free immunoassay based on the electron transfer through the multilayer films with the unique property of gold nanoparticles was presented using human IgG as the model analyte. The characterization of sensing interface was carried out, and the optimum experimental conditions and analytical performance were investigated in detail. The proposed analysis scheme not only exhibited excellent response performance but also circumvent the various problems associated with labeled immunosensor.

* Corresponding author. Tel.: +86 731 88822577; fax: +86 731 88822577.
E-mail addresses: wuzaisheng@163.com (Z.-S. Wu), rqyu@hnu.cn (R.-Q. Yu).

0039-9140/$ – see front matter © 2010 Elsevier B.V. All rights reserved.
doi:10.1016/j.talanta.2010.08.036

2. Experimental

2.1. Chemicals and apparatus

Human immunoglobulin G (human IgG), goat monoclonal anti-human IgG antibody, and bovine serum albumin (BSA) were purchased from Dingguo Biochemical Reagents (Changsha, PR China). Thionine and chloroauric acid ($HAuCl_4 \cdot 4H_2O$) came from Sinopharm Chemical Reagents (Shanghai, China). Trisodium citrate was obtained from Guangdong Taishan Chemicals (Guangdong, China). All chemicals were of analytical-reagent grade and used as received unless otherwise stated. The ultra-pure water (resistance > 18.2 MΩ cm) was used throughout the experiments.

Gold nanoparticles were prepared by the reduction of $HAuCl_4$ via the help of citrate, according to the previous method [23]. The proteins were dissolved in 10^{-2} mol L^{-1} phosphate buffered saline (PBS, pH 7.4) containing 0.3 mol L^{-1} NaCl, and stored at 4 °C until used.

Scanning electron microscopy (SEM) analysis was conducted using a JSM-5600LVmicroscope (JEOL Ltd., Japan). All the electrochemical detections were performed in a conventional three-electrode system consisted of sensing interface, saturated calomel reference electrode and platinum counter electrode, using CHI 760B electrochemical workstation (Shanghai, China).

2.2. Sensor fabrication

The gold electrode was pretreated according to the protocol reported in the previous work [24]. As shown in Scheme 1, the electropolymerization of the thionine monomer on the cleaned electrode surface was carried out in two steps [20]: first, the gold electrode was held under a constant potential of +1.5 V for 10 min in 10^{-2} mol L^{-1} phosphate buffered saline (PBS, pH 6.0) containing 10^{-3} mol L^{-1} thionine monomer, 0.1 mol L^{-1} KCl and 4×10^{-3} mol L^{-1} methylene blue (MB); second, CV scanning was conducted between −0.45 V and +0.15 V at 50 mV s^{-1}, with 25 cycles in the identical solution. Subsequently, the modified sensing surface was covered with 30 μL of gold nanoparticles solution and cultivated at room temperature in a water-saturated atmosphere for 4 h. Then, 10 μL of antibody solution was dropped onto the surface of the electrode and allowed to react for 1 h. To cover the non-specific sites, 10 μL of BSA solution (10 mg mL^{-1}) was dropped onto the electrode surface. After reacting for 1 h, the proposed sensing interface (PTH-MB/GNP/antibody electrode) for human IgG assay was obtained.

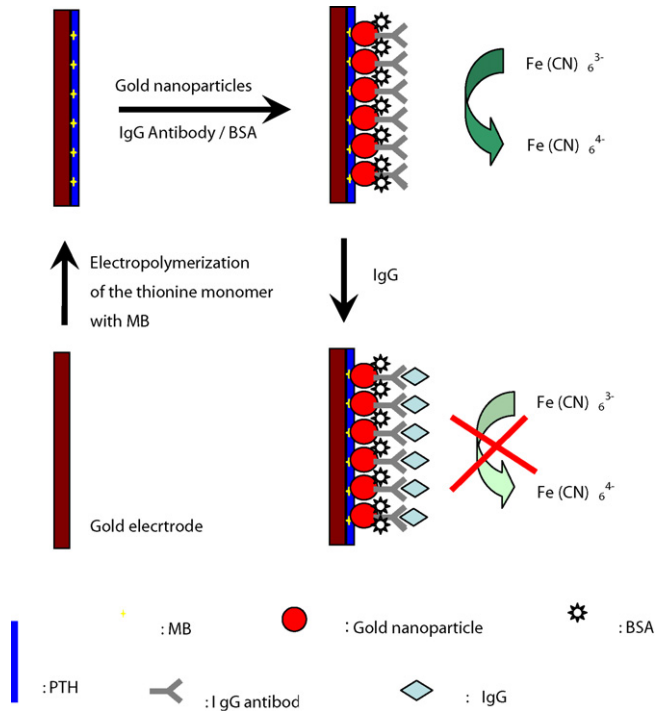

Scheme 1. Design of IgG sensing interface.

2.3. Electrochemical measurements

The different pulse voltammograms (DPVs) were recorded from 0.6 V to −0.2 V and the baseline-subtracted currents were used to evaluate the response characteristics of sensing interface. The AC impedance measurements were performed in the frequency range from 1 Hz to 100 kHz. Cyclic voltammetry (CV) measurements were scanned from 0.6 V to −0.6 V at 100 mV s^{-1}. All the electrochemical measurements were carried out in 10^{-2} mol L^{-1} PBS (pH 7.4) containing 0.1 mol L^{-1} KCl and 5×10^{-3} mol L^{-1} $K_3[Fe(CN)_6]/K_4[Fe(CN)_6]$ unless otherwise stated.

2.4. Detecting IgG

The samples with different antigen concentrations were dropped onto the as-prepared sensing interface (PTH-MB/GNP/antibody electrode), and allowed to immunoreact for 1 h. After rinsing thoroughly with ultra-pure water, the electrochemical measurements of the resulting electrode were carried out.

3. Results and discussion

3.1. Sensor fabrication

To fabricate the sensing interface for IgG detection, electropolymerization onto the gold electrode surface was conducted via potential scanning in TH/MB solution. As shown in Fig. 1, a typical cyclic voltammogram during the electropolymerization is observed. Due to the good conductivity of TH, the redox peak current increases with the increment of scan turns, indicating the growing process of PTH film on the gold surface, and then tends to be stable after 25 cycles, revealing that the gold electrode is

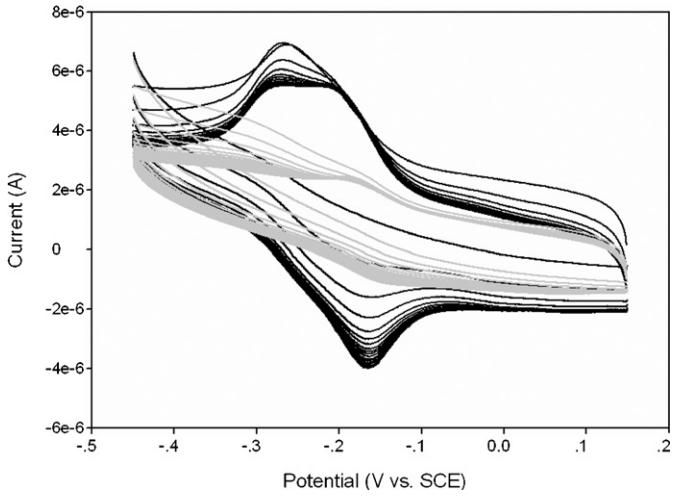

Fig. 1. The cyclic voltammograms of electropolymerization of thionine monomer onto a bare gold electrode in 10^{-2} mol L^{-1} PBS (pH 6.0) containing 10^{-3} mol L^{-1} thionine monomer and 0.1 mol L^{-1} KCl in the presence (outside) and absence (inside) of 4×10^{-3} mol L^{-1} MB.

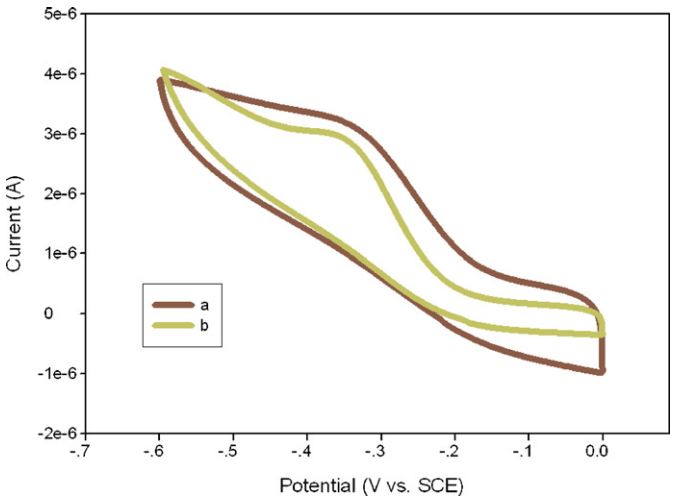

Fig. 2. The cyclic voltammograms of PTH film-modified electrode (a) and PTH-MB film-modified electrode (b) in 10^{-2} mol L^{-1} PBS (pH 7.4) containing 0.1 mol L^{-1} KCl.

almost saturated by the PTH film and further electropolymerization is hindered.

When adding MB to the deposition solution, the redox peak current relatively increases. We speculate that MB as an excellent electroactive substance improves the conductivity of the sensing interfaces. As shown in Fig. 2, the redox peak current of the PTH-MB electrode (b) is 9.967×10^{-7} A at voltage potential of −0.334 V, which is 113.8% more sensitive than that of the PTH electrode (a) (8.761×10^{-7} A) by potential scanning in 10^{-2} mol L^{-1} PBS containing 0.1 mol L^{-1} KCl. The resultant sensing interface is expected to improve the response performance of our analysis system.

The AC impedance characteristics of the modified interfaces were investigated. As shown in Fig. 3, no detectable change in the charge-transfer resistance (AC impedance) is obtained even after the formation of the electroactive polymer film (b), compared with the bare gold electrode (a). The conductivity also almost does not change when gold nanoparticles adsorb onto the surface of the PTH-MB film-modified electrode via the strong covalent bond between the amino groups and gold (c). The insulated protein layer formed on the modified gold electrode impedes the interfacial electron transfer, leading to an obvious increase in the resistance of the working interface (d). This demonstrates the accomplishment of antibody-based biorecognition interface.

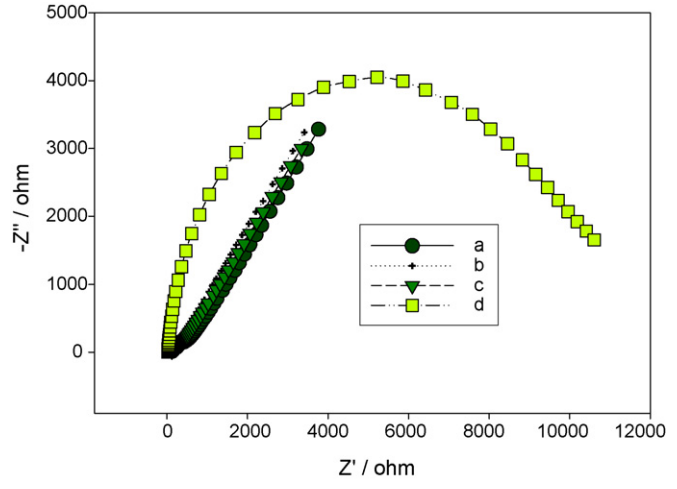

Fig. 3. The AC impedances of the sensing interfaces at different preparation stages: bare gold electrode (a); PTH-MB film-modified electrode (b); gold nanoparticle-modified electrode (c); antibody-immobilized electrode (d).

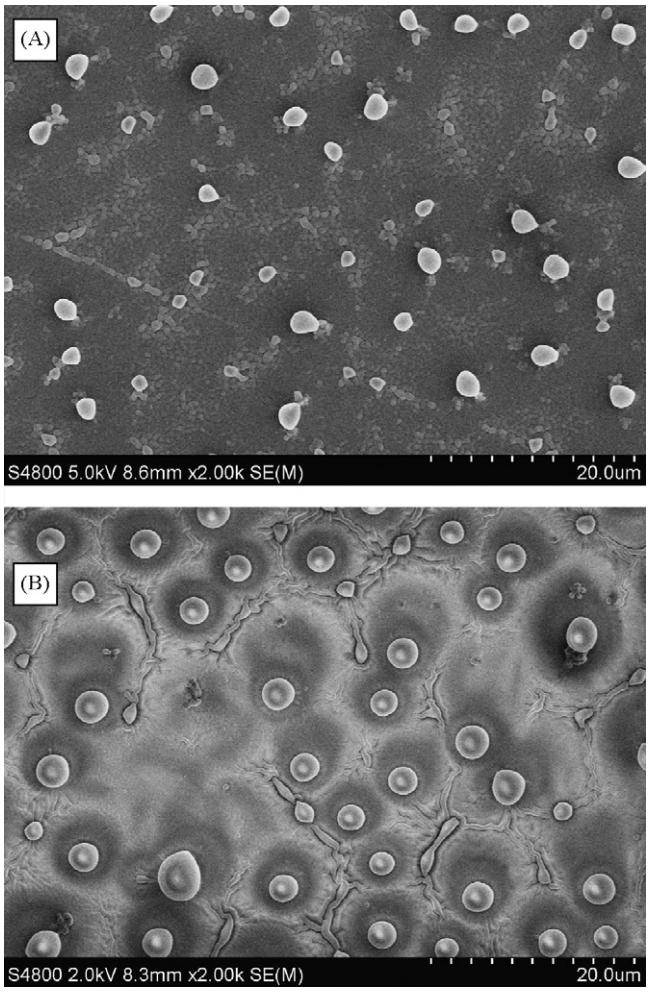

Fig. 4. The SEM images for the PTH-MB/GNP/antibody electrode before (A) and after (B) the addition of the antigen.

To confirm that the biorecognition reaction was successfully conducted, the morphology of the PTH-MB/GNP/antibody electrode before and after the addition of antigen was characterized using SEM. As shown in Fig. 4, the antibody molecules look like bright particles with the general size of 1–2 μm (A). After reacting with antigen, the particles grow bigger (2–3 μm) and look smoother (B) due to the lower conductivity. The difference of the two interfaces indicates the attachment of antigens, indicating the feasibility of our scheme.

Despite being immobilized successfully, the concentration of antibody directly affects the signal intensity corresponding to target molecule. Thus, the effect of antibody concentration on the current signal was investigated, and the results are shown in Fig. 5. The original antibody solution (10 mg mL^{-1}) was diluted with 10^{-2} mol L^{-1} PBS (pH 7.4) containing 0.3 mol L^{-1} NaCl to prepare a series of antibody solutions. The redox peak current increases with the increment of antibody concentration, and then reaches the highest at 3 mg mL^{-1}. The current signal gradually decreases at higher concentration. Due to the limited amount of loading sites on the sensing surface, the higher antibody concentration might increase the disorder in alignment of adsorbed antibody, hampering the following immunoreaction. Therefore, the antibody concentration of 3 mg mL^{-1} is chosen as the optimal in the present experiment.

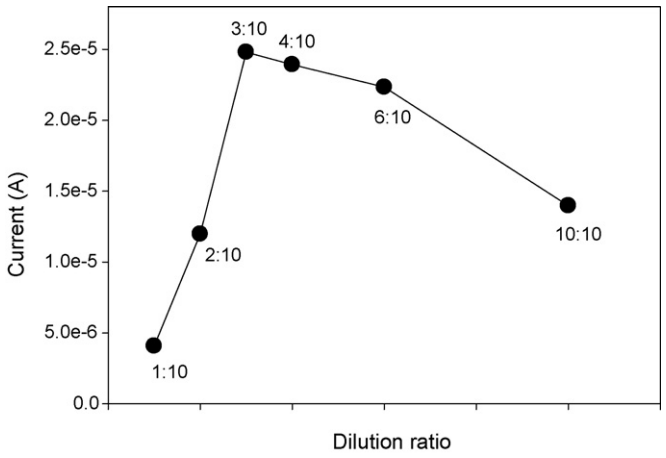

Fig. 5. Effect of the dilution ratio of antibody immobilized onto the gold nanoparticle-modified electrode on the signal intensity. The original antibody concentration was 10 mg mL^{-1}.

3.2. Amplification of electrochemical signal

To confirm the feasibility of our present proposal, two control sensing interfaces were prepared. The preparation of PTH/GNP/antibody electrode (electrode B) was the same as that of PTH-MB/GNP/antibody electrode (electrode A) described in Section 2.2 except without MB in the electrodeposition solution; PPD-MB/GA/antibody electrode (electrode C) chose glutaraldehyde (GA) as cross-linker instead of gold nanoparticles in the fabrication. As shown in Fig. 6, before the addition of IgG, electrode C presents only 29% of the current response provided by electrode A. After immunoadsorption of IgG on the sensing interface, the current change of electrode C is only 9% of that provided by electrode A. Compared with glutaraldehyde (GA), gold nanoparticles show better conductivity, more excellent biocompatibility and higher surface area-to-volume ratio. Therefore, electrode A provides higher sensitivity than electrode C. Electrode B provides only 57% (Fig. 6B line a) of the peak current (Fig. 6A line a) of electrode A before the addition of IgG. On the other hand, the current change of electrode B upon the immunoadsorption of IgG is only 44% of that of electrode A. We speculate that MB as an excellent electroactive substance is able to promote the interfacial electron transfer and improve the electrocatalytic reduction of ferricyanide [25], resulting in an enhanced current. In short, an improved response performance offered by the proposed sensing interface comes from the combination of MB and gold nanoparticles.

3.3. Response characteristics of electrochemical immunosensor

To assess the analytical performance of the proposed biosensor, a series of samples with different antigen concentrations were prepared and the DPVs were performed under the optimized experimental conditions. All the DPVs in the present section were the baseline-subtracted currents. As shown in Fig. 7, the current change (ΔI_{peak}) increases with the increment of IgG concentration within a certain range. The reason is that the redox reaction between Fe(II) and Fe(III) occurring on the electrode surface is closely related to the surface-adsorbed elements, and the increase in the amount of antigen immunoadsorpted on the sensing surface causes the decrement of the redox peak current. When the peak current change is plotted versus the logarithm of the target concentration, a linear relationship in the concentration ranging from 10 to 10^4 ng mL^{-1} is achieved, and the regression equation is $\Delta I_{peak} = 1.252 \times 10^{-5} \log C - 4.358 \times 10^{-6}$ with a correlation coefficient of 0.996 (as shown in Fig. 7B). The detection limit (defined as three times the standard deviation of the blank solution) is about 3 ng mL^{-1}. Such a good performance should be attributed to the striking change of the peak current originating from the immunoreaction between IgG and IgG antibody.

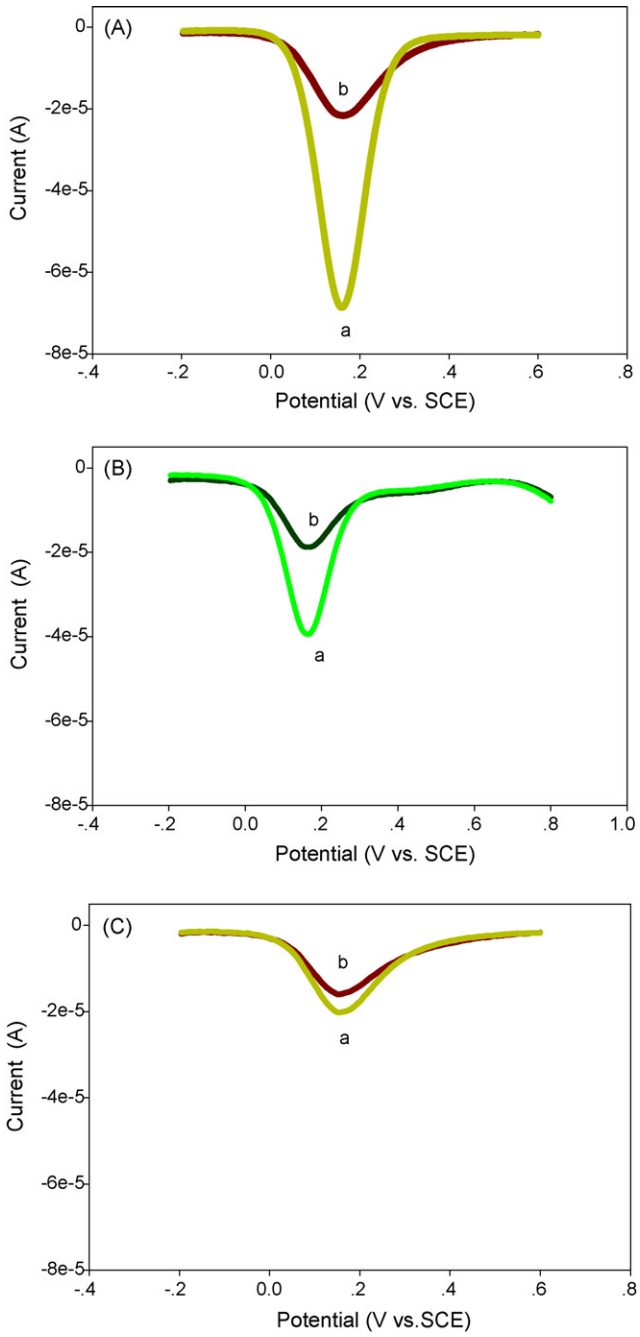

Fig. 6. Baseline-corrected DPVs of Fe $(CN)_6^{3-}$/Fe $(CN)_6^{4-}$ at sensing interfaces prepared by different methods before (line a) and after (line b) the addition of 1 μg mL^{-1} IgG. The working electrode used was PTH-MB/GNP/antibody electrode (A); PTH/GNP/antibody electrode (B); PTH-MB/GA/antibody electrode (C).

To test the applicability and reliability of the presented strategy, the recovery experiment of samples with different concentrations was carried out and the results were listed in Table 1. Recoveries in the range of 96.4–109.0% with the relative standard deviation of 7.4–9.1% are achieved ($n = 3$).

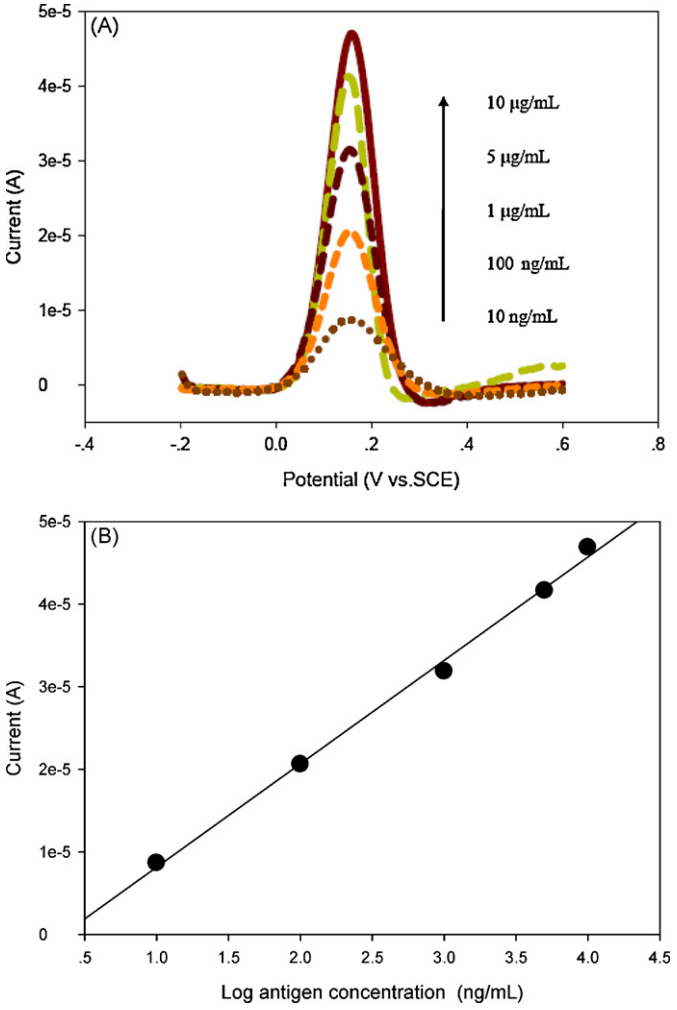

Fig. 7. The current response of the sensing system for detecting IgG at different concentrations (A); the linear relationship between the change of current response and log of IgG concentration (B).

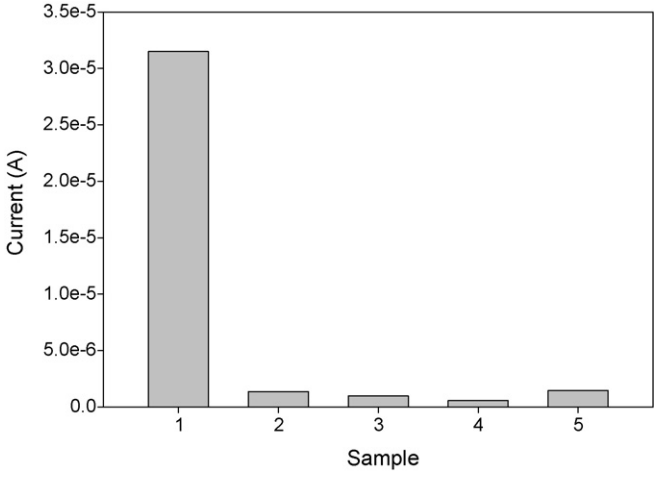

Fig. 8. The baseline-subtracted DPV response of the proposed sensing system after being exposed to five different proteins dissolved in 10^{-2} mol L^{-1} PBS (pH 7.4) containing 0.3 mol L^{-1} NaCl: (1) 1 μg mL^{-1} IgG; (2) 1 μg mL^{-1} HSA; (3) 1 μg mL^{-1} fibronectin; (4) 10 mg mL^{-1} BSA; (5) 36 μg mL^{-1} IgE.

Table 1
Recovery of IgG assay.

Sample	Added IgG (ng/mL)	Found IgG (ng/mL)	Recovery (%)	R.S.D. (%)
1	10.0	10.9	109.0	9.1
2	100.0	98.5	98.5	8.2
3	1000.0	963.6	96.4	7.4

3.4. Specificity

Selectivity is important for a presented sensor, in order to confirm that the current response was generated from antibody–antigen specific immunoreaction rather than non-specific adsorption, the affect of HSA (1 μg mL^{-1}), fibronectin (1 μg mL^{-1}), BSA (10 mg mL^{-1}) and IgE (36 μg mL^{-1}) was investigated under the same conditions. As shown in Fig. 8, compared with IgG (1 μg mL^{-1}), the current change induced by introduction of the four proteins could be negligible. That is to say, the present system reveals excellent selectivity.

4. Conclusion

A highly selective, label-free immunoassay based on the combination of the charge transport through the multilayer films and the unique properties of MB and gold nanoparticles has been presented. This approach can avoid various difficulties related with synthesizing the additional materials (e.g. reporters and signal amplifiers) or controlling and preserving the biological activity of enzymes. Given attractive performances, the proposed technique appears to provide a promising platform for the direct immunoassay of IgG or other biomolecules.

Acknowledgement

The work was financially supported by the National Natural Science Foundation (Grant 20775023) of China and Scientific Research Fund of Hunan Provincial Education Department (08A065).

References

[1] A. Loquet, B. Bardiaux, C. Gardiennet, C. Blanchet, M. Baldus, M. Nilges, T. Malliavin, A. Bockmann, J. Am. Chem. Soc. 130 (2008) 3579–3589.
[2] Y. Du, C. Chen, B. Li, M. Zhou, E. Wang, S. Dong, Biosens. Bioelectron. 25 (2010) 1902–1907.
[3] M. Kats, M.E.S. Germain, Anal. Biochem. 307 (2002) 212–218.
[4] X. Liu, Q. Dai, L. Austin, J. Coutts, G. Knowles, J. Zou, H. Chen, Q. Huo, J. Am. Chem. Soc. 130 (2008) 2780–2782.
[5] C. Xie, F. Xu, X. Huang, C. Dong, J. Ren, J. Am. Chem. Soc. 131 (2009) 12763–12770.
[6] I. Abdel-Hamid, P. Atanasova, A.L. Ghindilis, E. Wilkins, Sens. Actuators B 49 (1998) 202–210.
[7] M.F. Clark, A.N. Adams, J. Gen. Virol. 34 (1977) 475–483.
[8] J.P. Salvador, F. Sanchez-Baeza, M.P. Marco, Anal. Chem. 79 (2007) 3734–3740.
[9] Y. Zhuo, R. Yuan, Y. Chai, Y. Zhang, X.l. Li, Q. Zhu, N. Wang, Anal. Chim. Acta 548 (2005) 205–210.
[10] G. Jie, J. Zhang, D. Wang, C. Cheng, H.Y. Chen, J.J. Zhu, Anal. Chem. 80 (2008) 4033–4039.
[11] J. Zhang, J. Lei, C. Xu, L. Ding, H. Ju, Anal. Chem. 82 (2010) 1117–1122.
[12] F.F. Bier, E. Ehrentreich-Fijrster, R. Doelling, A.V. Eremenko, F.W. Scheller, Anal. Chim. Acta 344 (1997) 119–124.
[13] Z.H. Wang, G. Jin, Anal. Chem. 75 (2003) 6119–6123.
[14] N. Backmann, C. Zahnd, F. Huber, A. Bietsch, A. Pluckthun, H.P. Lang, H.J. Guntherodt, M. Hegner, C. Gerber, PNAS 102 (2005) 14587–14592.
[15] W. Liang, W. Yi, S. Li, R. Yuan, A. Chen, S. Chen, G. Xiang, C. Hub, Clin. Biochem. 42 (2009) 1524–1530.
[16] P. He, Z. Wang, L. Zhang, W. Yang, Food Chem. 112 (2009) 707–714.
[17] P. Ghosh, G. Han, M. De, C.K. Kim, V.M. Rotello, Adv. Drug Deliver. Rev. 60 (2008) 1307–1315.
[18] N. Wangoo, K.K. Bhasin, R. Boro, C. Raman Suri, Anal. Chim. Acta 610 (2008) 142–148.
[19] M.C. Daniel, D. Astruc, Chem. Rev. 104 (2004) 293–346.
[20] R. Yang, C. Ruan, W. Dai, J. Deng, J. Kong, Electrochim. Acta 44 (1999) 1585–1596.

[21] V.E. Nicotra, M.F. Mora, R.A. Iglesias, A.M. Baruzzi, Dyes Pigments 76 (2008) 315–318.
[22] Y. Ding, X. Zhang, X. Liu, R. Guo, Langmuir 22 (2006) 2292–2298.
[23] M.F. Huang, Y.C. Kuo, C.C. Huang, H.T. Chang, Anal. Chem. 76 (2004) 192–196.
[24] Z.S. Wu, M.M. Guo, S.B. Zhang, C.R. Chen, J.H. Jiang, G.L. Shen, R.Q. Yu, Anal. Chem. 79 (2007) 2933–2939.
[25] E.M. Boon, D.M. Ceres, T.G. Drummond, M.G. Hill, J.K. Barton, Nat. Biotechnol. 18 (2000) 1096–1102.